

Correction for Blending Problem in Gravitational Microlensing Events by Using Hubble Space Telescope

Cheongho Han
Dept. of Astronomy & Space Science,
Chungbuk National University, Cheongju, Korea 360-762

Received _____; accepted _____

arXiv:astro-ph/9704212v1 22 Apr 1997

ABSTRACT

The biggest uncertainty in determining microlensing parameters comes from the blending of source star images because the current experiments are being carried out toward very dense star fields: the Galactic bulge and Magellanic Clouds. The experiments try to correct the blending effects for individual events by introducing an additional lensing parameter, the residual flux, but this method suffers from very large uncertainties in the derived lensing parameters due to the degeneracies among the parameters. In this paper, I propose to use the *Hubble Space Telescope* (*HST*) to correct blending effects. With the high resolving power of the *HST* combined with the color information from ground-based observations, one can uniquely identify the lensed source star in the blended seeing disk, and thus the uncertainty in the derived time scale can be significantly reduced.

Subject headings: The Galaxy — gravitational lensing — dark matter — Stars: low-mass, brown dwarfs

submitted to *The Astrophysical Journal*: April 21, 1996
Preprint: CNU-A&SS-01/97

1. Introduction

Presently, four groups are searching for Massive Astronomical Compact Halo Objects (MACHOs) by observing light variations of stars caused by gravitational microlensing: MACHO (Alcock et al. 1995, 1997), EROS (Aubourg et al. 1993; Ansari et al. 1997), OGLE (Udalski et al. 1994a), and DUO (Alard 1996a). From microlensing experiments toward Large Magellanic Cloud (LMC), one can constrain the MACHO dark-matter fraction in the Galactic halo. Experiments toward the Galactic bulge provide a new probe of low-mass stellar objects in the Galaxy.

To maximize the event rate, the searches are being carried out toward very dense star fields, where the images of stars are severely blended with one another, and thus observation is limited by crowding. When an event in such a dense field is monitored, the observed light curve is affected by the light from stars that are not lensed: blending effect. If the effect is not properly corrected, the MACHO dark-matter fraction in the Galactic halo, determined from the lensing optical depth, will be subject to great uncertainties. In addition, blending makes identification of the major lens population difficult because it causes the determined time scale shorter than the true value. The lensing optical depth represents the probability for a single source star to be lensed and is observationally determined by

$$\tau = \frac{\pi}{2N_*T} \sum_{i=1}^{N_{\text{event}}} \frac{t_{\text{E},i}}{\epsilon(t_{\text{E},i})}, \quad (1.1)$$

where ϵ is the detection efficiency, T is the total observation time, and N_* and N_{event} are the total numbers of monitored source stars and actually detected events, respectively. The Einstein time scale is related to the physical parameters of a lens by

$$t_{\text{E}} = \frac{r_{\text{E}}}{v}; \quad r_{\text{E}} = \left(\frac{4GM_L D_{\text{ol}} D_{\text{ls}}}{c^2 D_{\text{os}}} \right)^{1/2}, \quad (1.2)$$

where r_{E} is the Einstein ring radius, v is the transverse speed of the lens relative to the observer-source line of sight, D_{ol} , D_{ls} , and D_{os} are the distances between the observer, lens, and the source, and M_L is the mass of the lens.

When one of multiple stars in an *effective seeing disk*, the maximum undistinguishable separation between images, is gravitationally lensed, the measured flux is the sum of flux from the lensed star and residual flux from blended stars,

$$F = F_{0,i} A + B; \quad B = \sum_{j \neq i} F_{0,j}. \quad (1.3)$$

Here $F_{0,i}$ is the flux of the lensed star before or after gravitational amplification, and the amplification is related to lensing parameters by

$$A(u) = \frac{u^2 + 2}{u(u^2 + 4)^{1/2}}; \quad u = \left[\beta^2 + \left(\frac{t - t_0}{t_{\text{E}}} \right)^2 \right]^{1/2}. \quad (1.4)$$

where u is the lens-source separation in units of r_{E} , β is the impact parameter, and t_0 is the time of maximum amplification.

There are two types of blending in microlensing. The first case occurs when a star brighter than the detection limit, which is set by crowding, is lensed and the measured flux is affected by residual flux from other blended stars fainter than the detection limit. The term ‘blending’ in microlensing usually refers to this case, and I will refer to this type of blending as “regular blending”. The other type of blending occurs when one of several faint stars below the crowding limit is lensed and its flux is associated with the flux from other stars in the effective seeing disk. In this case, the event appears seemingly with the brightest star as the source star because the lensed star is not resolved and thus not registered in the template plate. Due to the second type of blending, the relative probability of detecting low-amplification events (after proper efficiency correction) is higher than random distribution which is expected for unblended events. Therefore, the second type of blending is often referred as “amplification bias” (Blandford & Narayan 1992; Narayan & Wallington 1994; Nemiroff 1994; Han 1997; Alard 1996b).

Blending, both regular blending and amplification bias, affects the results of the lensing experiments in various ways. First, blending restricts one to detecting only events with amplifications high enough to overcome the threshold residual flux level contributed by the blended stars in the effective seeing disk. For the detection of an event with a source star flux $F_{0,i}$, the amplification should satisfy the condition

$$\frac{A_{\min}F_{0,i} + B}{F_{0,i} + B} \geq 1.34, \quad (1.5)$$

resulting in the minimum amplification for detection of

$$A_{\min} = \frac{1.34(F_{0,i} + B) - B}{F_{0,i}}. \quad (1.6)$$

Secondly, even for detected events one measures only the portion of the light curve which is above the threshold. Since this part of the light curve mimics that of a shorter time scale event, what is measured is not the Einstein time scale t_E , but the effective time scale t_{eff} . The two time scales are related by

$$t_{\text{eff}} = \eta(\beta)t_E; \quad \eta(\beta) = \left[\beta_{\max}^2 - \beta^2 \right]^{1/2} \quad (1.7)$$

where β_{\max} is the maximum allowed impact parameter for detection and it is related to the minimum required amplification by

$$\beta_{\max} = \left[2 \left(1 - A_{\min}^{-2} \right)^{-1/2} - 2 \right]^{1/2}. \quad (1.8)$$

Therefore, the observed time scale distribution is systematically shifted toward shorter time scales, i.e., $\eta \leq 1.0$. In particular, the time scales of amplification-biased events are much more seriously affected compared to those of regular-blended events because of relatively much higher residual fluxes. Since the lens mass scales as $M \propto t_E^2$, the mass determined from the measured time scale will be underestimated and the lens population will be misinterpreted. For example, blended events caused by main-sequence stars will be confused with unblended events caused by brown dwarfs. The other important effect of amplification bias is that the

optical depth to microlensing will be significantly overestimated because events are generated by all stars, both resolved and unresolved, while τ is determined from only the resolved stars (Han 1997). Therefore, if the blending is not properly corrected, the MACHO dark matter fraction of the Galactic halo will be seriously overestimated.

Although there have been several methods proposed to correct the blending problem, they are either applicable to limited cases, suffers from large uncertainties in the determined lens parameters, or they are statistical not on individual event basis. Currently, experiments try to correct the blending effects by introducing an additional lensing parameter, i.e., the residual flux B , into the light-curve fitting process (Alcock et al. 1997). However, this method suffers from increased uncertainties in derived lensing parameters due to the degeneracies among them and it sometimes results in physically unrealistic results, e.g., negative residual flux (M. R. Pratt 1996, private communication). A shift of star’s image centeroid can be used to identify the lensed source star (Alard 1996a), but this method is applicable only for a special event in which the template star is widely separated from a lensed star. One can correct the blending effects statistically if the luminosity function of stars well below the detection limit can be constructed (Han 1997), but in this case we lose information about individual events. Therefore, other methods should be explored.

In this paper, I propose to use the *Hubble Space Telescope* (*HST*) to correct blending effects in gravitational microlensing experiments. With the high resolving power of the *HST* combined with color information obtained from ground-based observation, one can uniquely identify the lensed source star in the effective seeing disk, and thus can significantly reduce the uncertainty in the derived time scale.

2. Fraction of Faint Events

The fields toward which the microlensing experiments are being carried out are very crowded. To estimate the average number of stars blended in the effective seeing disk of a star, I construct a model luminosity function (LF) of the stars in the galactic bulge field toward which the blending is most severe. I adopt the LF determined by J. Frogel (private communication) for stars brighter than the ground detection limit of $I_0 = 18.2$. For fainter stars in the range $18.2 \leq I_0 \leq 22.4$, I adopt the LF determined from *HST* observation by Light, Baum, & Holtzman (1997). For the part of LF even fainter than $I_0 = 22.4$, I adopt the LF of stars in the solar neighborhood which is determined by Gould, Bahcall, & Flynn (1996). The finally constructed LF is shown in Figure 1(a). In the figure, the LF is normalized for stars in an effective seeing disk of size $1''.5$.¹ According to the model LF, there will be ~ 36 stars in average in this effective seeing disk. Among them, the number of stars brighter than the detection limit comprises just ~ 0.75 , and majority of them are stars fainter than the detection limit and thus cannot be resolved.

¹ The average seeing of the current experiment is $\sim 2''$. However, if the angular separation between the lensed object and the template image is wide enough, the blending effect can be noticed by the shift of image centroid. I, therefore, set the effective size of unseparable seeing disk to be $\theta_{\text{eff}} = 1''.5$.

Among these stars in the effective seeing disk, the important source of blending comes from stars that are ~ 2 mag below the ground observation detection limit. In the dense region of the galactic bulge, each resolved bright template star works effectively as multiple source stars due to amplification bias. The effective number of source stars for a single template star with a flux F_t is determined by

$$n_{\text{eff}} = 1 + \int_0^{F_t} dF \Phi(F) \beta_{\text{max}}(F_t, F) \langle \epsilon(t_{\text{eff}}) / \epsilon(t_{\text{E}}) \rangle, \quad (2.1)$$

where $\Phi(F)$ is the LF of stars in the field, and the factor $\langle \epsilon(t_{\text{eff}}) / \epsilon(t_{\text{E}}) \rangle$ is introduced to account for the decrease in the detection limit for shorter time scales. Then the total number of effective source stars is obtained by integrating equation (2.1) over all stars brighter than the detection limit (F_{DL});

$$\begin{aligned} N_{\text{eff}} &= \int_{F_{\text{DL}}}^{\infty} dF_t n_{\text{eff}} \Phi(F_t) \\ &= \int_{F_{\text{DL}}}^{\infty} dF_t \Phi(F_t) + \int_{F_{\text{DL}}}^{\infty} dF_t \Phi(F_t) \int_0^{F_t} dF \Phi(F) \beta_{\text{max}}(F_t, F) \langle \epsilon(t_{\text{eff}}) / \epsilon(t_{\text{E}}) \rangle. \end{aligned} \quad (2.2)$$

Finally, the distribution of effective source star brightness of microlensing events is obtained by differentiating N_{eff} by F ;

$$dN_{\text{eff}}(F) = \Phi(F_t) dF_t + \int_{F_{\text{DL}}}^{\infty} dF_t \Phi(F_t) [\Phi(F) \beta_{\text{max}}(F_t, F) \langle \eta(t_{\text{eff}}) / \eta(t_{\text{E}}) \rangle dF]. \quad (2.3)$$

In equation (2.3), the first term represents the LF of template stars, while the second term accounts for the additional source stars due to amplification bias.

For the computation of $dN_{\text{eff}}(F)$, I assume the detection efficiency is related to the time scale by a power law: $\epsilon \propto t_{\text{eff}}^p$. Since the lensing events caused by amplification bias have very short time scales ($\lesssim 10$ days) where the dependence of detection efficiency to time scale is close to linear, I adopt $p = 1$. With this approximation and the model LF, the brightness distribution of effective source stars is computed by equation (2.3) and shown in Figure 1(b). One finds the contribution to the total events by the amplification-biased events is important; they comprise $\sim 40\%$ of the total events. One arrives at a similar result for a different model of detection efficiency; for the case $p = 1/2$, $\sim 50\%$ of the total events are amplification biased [see Figure 1(c)]. One also finds that most of all these amplification-biased events comes from the part of the LF which is ~ 2 magnitudes below the detection limit, i.e., $18.2 \lesssim I_0 \lesssim 20$ (shaded regions in Figure 1). According to the model LF there are ~ 4 such stars in each effective seeing disk. There will be additional numerous very faint stars in the same effective seeing disk; ~ 30 stars fainter than $I_0 \leq 20$. However, the contribution to the total event rate by these very faint stars will be negligible (see § 4.1).

3. Correction for Amplification-Biased Events

In previous section, I showed that the contribution to the total microlensing events by faint blended source stars is substantial, and these sources mainly come from ~ 2 magnitudes below the detection limit imposed by crowding limit. In this section I show that most of these

faint source stars can be resolved and precise measurements of their fluxes can be made by using *HST* (see § 3.1). Once these stars are resolved in a single pair of *HST* images which are taken after events, one can isolate the lensed source star from other blended stars by using the color changes observed during the event from the ground. This can be done by comparing the observed color curve to the one expected when each candidate source star is assumed to be the lensed source (see § 3.2).

3.1. Resolving Faint Source Stars

The *HST* delivers essentially diffraction-limited images (with a seeing of $\theta_{\text{see}} \sim 0''.1$ in *I* band), and thus it has more than 100 times resolving power than the observations taken under favorable conditions from the ground ($\theta_{\text{see}} \gtrsim 1''$). Then source star detection is no longer limited by crowding but only by photon statistics. Therefore, the important sources of blending, stars with ~ 2 magnitudes below the detection limit, can be easily resolved and precise measurement of their unamplified fluxes can be made with a few minutes of post-event *HST* observation, i.e., with a photometric precision of $\lesssim 2\%$, corresponding to a signal-to-noise ratio of $S/N \gtrsim 50$ for $I = 24$ star.

Since the proposed *HST* observation is required only to resolve individual stars in the effective seeing disk and measure their brightnesses not to obtain lensing event light curve, it can be carried out after events. However, the *HST* Wide Field Planetary Camera 2 (WFPC2) can cover only 3.25 arcmin^2 of sky, while the area covered by the microlensing experiments is in scales of several deg^2 . Therefore, observations are required for individual source stars. In addition, multiple exposures will be occasionally required for some bright sources to prevent saturation of images. The required observation time will be ~ 10 min in each band, and thus it will take slightly less than an hour including telescope operating time for each source star. Since events are detected at the rate $\gtrsim 50 \text{ yr}^{-1}$, the required *HST* observation time will be $\sim 50 \text{ hr yr}^{-1}$.

3.2. Isolating Lensed Source Star

If the lensed source is identified and its flux is known, the precision of the time scale determination will be significantly improved. To show the improvement in the precision of time scale determination with known source brightness, I carry out simulation of a representative event toward the galactic bulge where the blending is most severe. In the simulation, the ground-based observation is assumed to use 1.27m telescope with a dichroic beam splitter to give simultaneous imaging in both *V* and *R* bands. The CCD camera can detect $25 \text{ photons s}^{-1}$ with a 1m telescope for $V = 20$ star. This ground observation strategy is similar to that of MACHO group (Alcock 1996). There are four stars in an effective seeing disk with an angular radius $\theta_{\text{eff}}/2$; $\theta_{\text{eff}} = 1''.5$. The *V*- and *R*-band magnitudes of these stars are chosen based on the stellar distribution in the color-magnitude diagram provided by Alcock et al. (1997) and from the model LF, and they are listed in Table 1. In the table, each star is designated by $i = 1, 2, 3,$ and 4 according to their *V*-band brightnesses. Among these stars, the truly lensed source is $i = 2$ star, and the event has an observed effective time

scale of $t_{\text{eff}} = 16.5$ days. I assume the flux of the blended image is measured with a moderate photometric precision of $f = 5\%$ during the time span of $-3t_{\text{eff}} \leq t \leq 3t_{\text{eff}}$. The image is monitored twice per night, and thus the total number of data points is $6 \times 16.5 \times 2 \sim 200$.

To correct the blending effect caused by the amplification bias, one should know which star among all stars in the effective seeing disk is lensed. Theoretically, it is possible to determine the source star flux from the shape of the light curve by introducing the residual flux B as an additional parameter in the light-curve fitting process. However, the increase in the number of parameters results in severe degeneracy problem; with very different source star brightnesses different combinations of other lensing parameters can produce very similar light curves. This degeneracy in lensing parameters is well illustrated in Figure 2(a) and 2(b). In the figure, each light curve is obtained by fitting the model light curve to the observed one under the assumption that each star in the effective seeing disk is the lensed source star. One finds that although the lensing parameters are very different with one another, the shapes of the light curves are very similar, resulting in very similar effective time scales of $t_{\text{eff}} \sim 16.5$ days. The best-fitting lensing parameters of individual light curves are listed in Table 1.

More practical method for the isolation of the lensed source star is provided by measuring the color changes accompanied in blended events. In Figure 2(c), I show the expected *color curves*, color changes as a function of time, expected for individual candidate source stars. For our example case where $i = 2$ star is the lensed source, the color differences at the peak of the curves from those of other curves range 0.05-0.15 magnitudes. These differences are large enough to be easily measured from ground-based observation. Better photometry from the ‘Early Warning system’ (Udalski et al. 1994b) and ‘Alert system’ (Pratt et al. 1996) will make it possible to measure even smaller color differences.

3.3. Precise Time Scale Determination

Then how much does the precision of the time scale determination improve with the proposed method compared to the conventional one. For this comparison, I first compute the uncertainty of the time scale t_E determined by using the conventional method of correcting blending effect: four-parameter fitting. For this estimation, the observed light curves of the example events is fitted, including B , by using the relations (1.3) and (1.4), and the resulting values of χ^2 as functions of t_E and $F_{0,i}$ are shown as a contour map in Figure 3. In the fitting process, I let the values of β and t_0 vary so that the model curves under fixed values of $(t_E, F_{0,i})$ fit best to the observed one. The values of χ^2 are computed by

$$\chi^2 = \sum_{i=1}^{N_{\text{pt}}} \frac{(N_{\text{T}} - N_{\text{O}})^2}{(fN_{\text{T}})^2}, \quad (3.3.1)$$

where

$$\begin{cases} N_{\text{pt}} = 200 & \text{the number of data points} \\ N_{\text{T}}(t) & \text{the photon counts of the model light curve} \\ N_{\text{O}}(t) & \text{the measured photon counts} \\ f = 5\% & \text{the photometric precision of ground-based observation.} \end{cases}$$

In Figure 3, the contours are drawn at the levels of $\chi^2 = 1.0, 4.0, \text{ and } 9.0$, i.e., $1\sigma, 2\sigma,$ and 3σ levels, from inside to outside, and the uncertainties of the recovered time scales for

corresponding levels are listed in Table 2. One finds that when the source flux is not known, the uncertainty of the time scale is very large. For our example event, the uncertainty of the obtained time scale is $28.1^{\text{d}} \leq t_{\text{E}} \leq 1412.5^{\text{d}}$ measured at 1σ level while the true value is $t_{\text{E}} = 51.6^{\text{d}}$. On the other hand, if the lensed source star is identified from *HST* observation and its brightness is known, the uncertainty in the recovered time scale decreases significantly. For the example event, the uncertainty of the recovered time scale is $47.7^{\text{d}} \leq t_{\text{E}} \leq 69.2^{\text{d}}$ measured at the same level.

4. Further Considerations

4.1. Very Faint Source Events

For an event in which the lensed source is very faint, it will be difficult to detect the source star in a short exposure post-event *HST* observation. Even if these very faint stars are resolved with a deep *HST* image, identifying the lensed source star will be difficult due to mainly two reasons. First, there are too many such faint stars in the effective seeing disk, i.e., $\gtrsim 10$ stars in the range $20 \leq I_0 \leq 23$ according to the model LF. Secondly, the stellar type of these stars is mostly main sequence stars with similar colors. Therefore, it will be difficult to identify the lensed source star by using the color changes during the event. In addition, even if the spectral types are quite different, the expected color changes from these faint star event will be small.

However, the contribution to the event rate by these very faint stars will be small. This is because to be detected the star should be highly amplified, and thus rare. When the efficiency model $\epsilon(t_{\text{eff}})/\epsilon(t_{\text{E}}) = \eta$ is adopted, very faint source events with source star brightnesses $I_0 \geq 21$ comprise $\lesssim 5\%$ of the total events.

4.2. Blending by Binary Stars

Another complexity of blending arises when the source is composed of binary stars. Source might exhibit the binary nature when both components are lensed, but this case is very rare (Griest & Hu 1992). Typically, only one of the components are lensed and others works as stars contributing to the background flux: binary blending.

However, it is still possible to estimate the fraction of binary-blended events statistically. Let N_{field} be the number of events blended by field (single) stars, and most of them will be identified from *HST* observations. The remaining events that exhibit the effects of blending, but whose sources were not identified are most likely caused by binary blending. Therefore, one can determine the binary-blended event fraction by

$$f_{\text{bi}} = \frac{N_{\text{bi}}}{N_{\text{tot}}}; \quad N_{\text{bi}} = N_{\text{tot}} - N_{\text{field}}. \quad (4.2.1)$$

Here N_{tot} is the total number of blended events by both binary companions and field stars, while N_{bi} is the number events blended by only binary companions. Therefore, *HST* observations of events that are blended by unrelated field stars can be bootstrapped to

yield statistical estimation of binary-blended events. In addition, most binary systems are composed of one bright and the other relatively very faint star, causing minimal blending effects.

I acknowledge precious discussions with A. Gould.

REFERENCES

- Alard, C. 1996a, in Proc. IAU Symp. 173, Astrophysical Applications of Gravitational Lensing, ed. C. S. Kochanek & J. N. Hewitt, (Dordrecht: Kluwer), 215
- Alard, C. 1996b, A&A, submitted
- Alcock, C., et al. 1995, ApJ, 445, 133
- Alcock, C., et al. 1997, ApJ, 479, 119
- Ansari, R., et al. 1997, A&A, 314, 94
- Aubourg, E., et al. 1993, Msngr, 72, 20
- Blandford, R., & Narayan, R. 1992, ARA&A, 30, 311
- Gould, A., Bahcall, J. A., & Flynn, C. 1996, ApJ, 465, 759
- Griest, K., & Hu, W. 1992, ApJ, 397, 362
- Han, C. 1997, ApJ, 484, 000
- Light, R. M., Baum, W. A., & Holtzman, J. A., 1997, in preparation
- Narayan, R., & Wallington, S. 1994, in Proc. 31st International Liege Colloquium: Gravitational Lensing in the Universe (Liege: Inst. d'Astrophysique), 217
- Nemiroff, R. J. 1994, ApJ, 435, 682
- Udalski, A., et al. 1994a, AcA, 44, 165
- Udalski, A., et al. 1994b, AcA, 44, 227

| event | lensed star | | lensing parameters | | | |
|---------|-------------|-------------|--------------------|---------|-------|-------------------------|
| | V_i (mag) | R_i (mag) | t_E (days) | β | t_0 | t_{eff} (days) |
| $i = 1$ | 17.5 | 16.5 | 21.9 | 0.3 | 0 | 16.2 |
| $i = 2$ | 19.0 | 18.3 | 51.6 | 0.1 | 0 | 16.5 |
| $i = 3$ | 19.3 | 18.5 | 63.4 | 0.08 | 0 | 16.5 |
| $i = 4$ | 20.0 | 19.2 | 113.3 | 0.05 | 0 | 17.0 |

Table 1: The V - and R -band magnitudes of stars in the effective seeing disk for the example event. In the effective seeing disk of the template star $i = 1$, there are other three faint blended stars. Among these stars, the truly lensed source is $i = 2$ star, and the event has an observed time scale of $t_{\text{eff}} = 16.5$ days. Also listed are the lensing parameters which can produce very similar light curves to the observed one under the assumption that each star is the lensed source.

| uncertainties level | with conventional method | with known source star brightness |
|---------------------|---|--|
| 1σ | $1.45 \leq \log t_E \leq 3.15$ ($28.1^{\text{d}} \leq t_E \leq 1412.5^{\text{d}}$) | $1.65 \leq \log t_E \leq 1.84$ ($44.7^{\text{d}} \leq t_E \leq 69.2^{\text{d}}$) |
| 2σ | $1.30 \leq \log t_E \leq 3.30$ ($20.0^{\text{d}} \leq t_E \leq 1995.2^{\text{d}}$) | $1.56 \leq \log t_E \leq 1.95$ ($36.3^{\text{d}} \leq t_E \leq 89.1^{\text{d}}$) |
| 3σ | $1.13 \leq \log t_E \leq 3.60$ ($13.5^{\text{d}} \leq t_E \leq 3981.1^{\text{d}}$) | $1.45 \leq \log t_E \leq 2.05$ ($28.2^{\text{d}} \leq t_E \leq 112.2^{\text{d}}$) |

Table 2: Uncertainties in the determined time scale of the example event. The uncertainties in the second column are determined by the conventional method of four-parameter fitting, and they are compared to those, in the last column, determined with known source star brightness from *HST* observation.

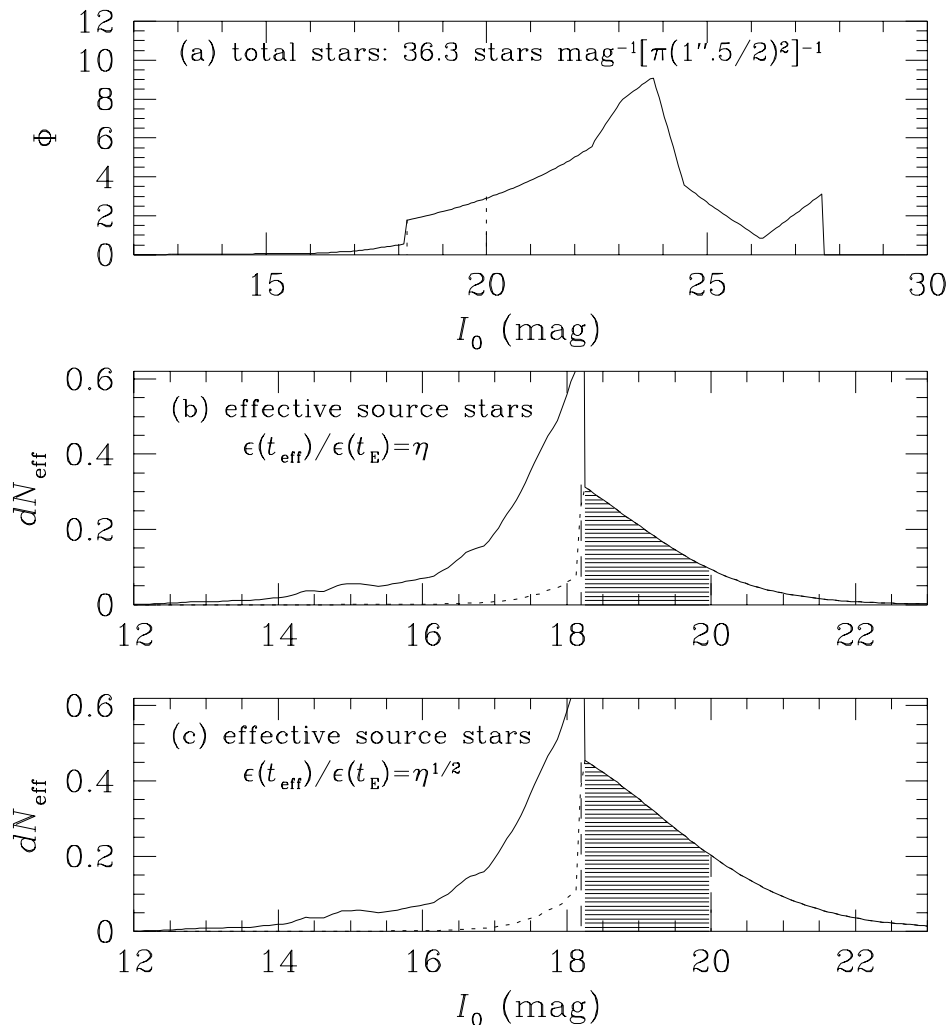


Figure 1: (a): The model I -band luminosity function of stars in the galactic bulge field. There are totally $\sim 36 \text{ stars mag}^{-1}$ inside the effective seeing disk of $\theta_{\text{eff}} = 1''.5$. (b): The expected effective source star brightness distribution under the model that the detection efficiency is related to the time scale by $\epsilon(t_{\text{eff}})/\epsilon(t_{\text{E}}) = t_{\text{eff}}/t_{\text{E}} = \eta$. In this case the amplification-biased events comprises $\sim 40\%$ of the total events. (c): The distribution of effective source star brightness when $\epsilon(t_{\text{eff}})/\epsilon(t_{\text{E}}) = \eta^{1/2}$. Under this model the fraction of the amplification-biased events to the total events is $\sim 50\%$.

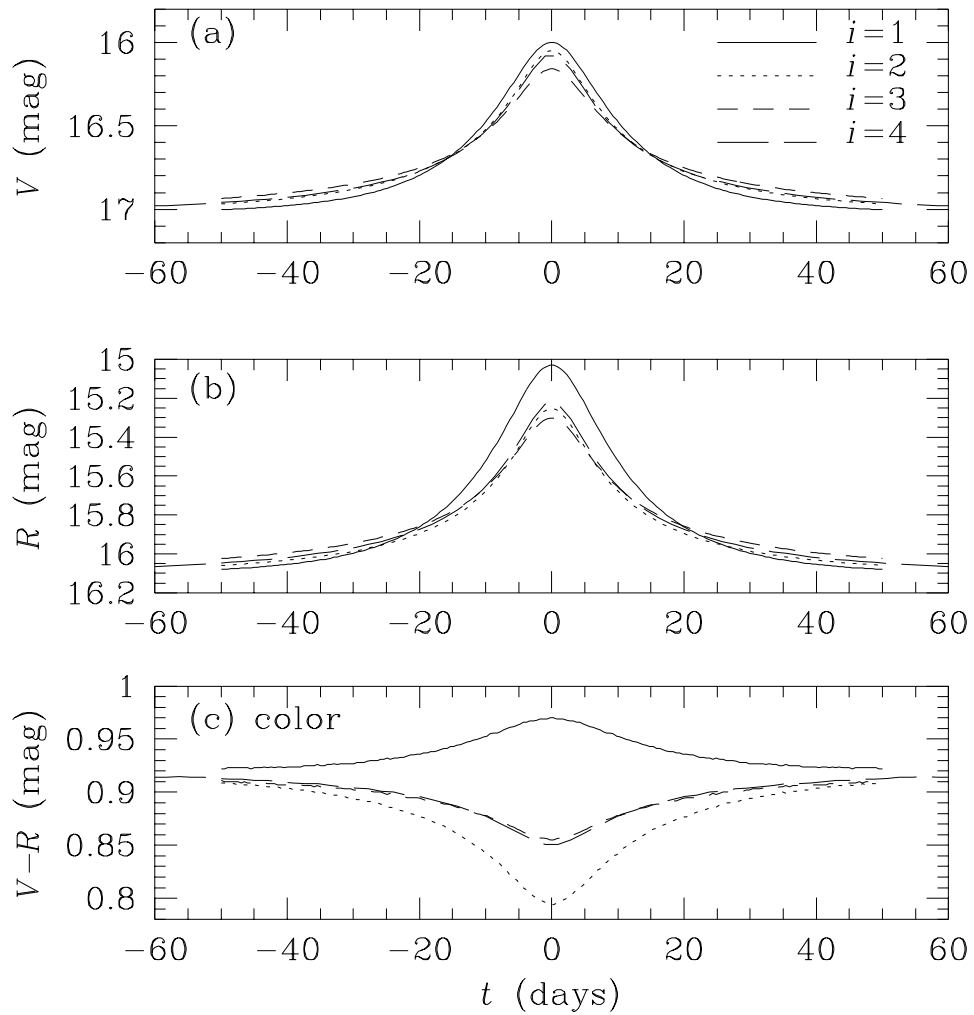


Figure 2: The best fitting V - and R -band, (a) and (b) respectively, light curves to the observed one when individual stars in the effective seeing disk in Table 1 are assumed to be the lensed source. Regardless of the source star brightnesses, all light curves results in similar effective time scale of $t_{\text{eff}} = 16.5$ days. Also shown, in panel (c), are the corresponding color curves for individual candidate source star events.

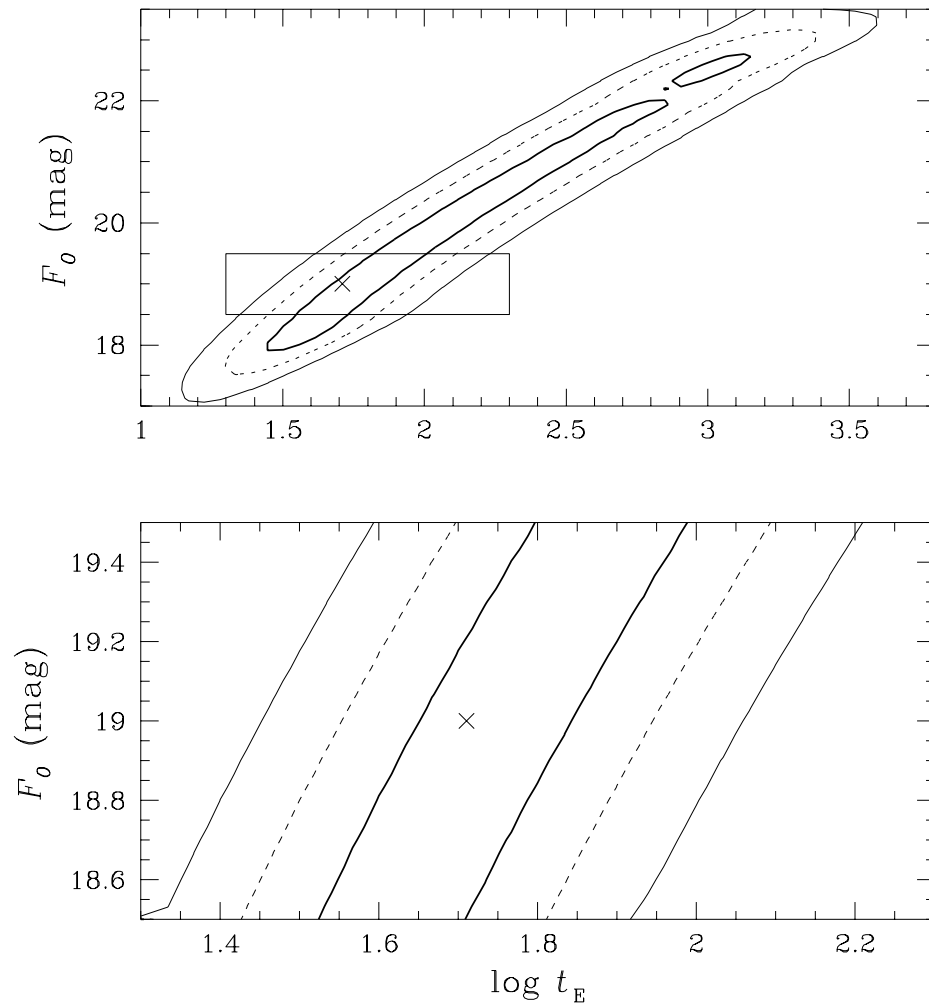


Figure 3: The uncertainties of the best-fitting source star brightness and time scale for the example event. The fit for a given value of t_E and F_0 is measured by χ^2 and its value is shown as a contour map. The contours are drawn at the levels of $\chi^2 = 1.0, 4.0,$ and 9.0 from inside to outside. The region of parameter space in a small box in the upper panel is expanded and shown in the lower panel. One finds that with known source flux the uncertainty of the derived time scale significantly reduces. The “ \times ” mark represents the position of true source star brightness and time scale.